Turbulence and Control of Wind Farms

Carl Shapiro[1,2], Genevieve M. Starke[1], and Dennice F. Gayme[1]

[1]Department of Mechanical Engineering, Johns Hopkins University, Baltimore, MD, 21212; email: dennice@jhu.edu
[2]AAAS Science & Technology Policy Fellow, U.S. Department of Energy Building Technologies Office, Washington, D.C. 20585.

Xxxx. Xxx. Xxx. Xxx. YYYY. AA:1–26

https://doi.org/10.1146/((please add article doi))

Keywords

Wind energy, wind farm control, wake models, state estimation, renewable energy

Abstract

The dynamics of the turbulent atmospheric boundary layer (ABL) play a fundamental role in wind farm energy production, governing the velocity field that enters the farm as well as the turbulent mixing that regenerates energy for extraction at downstream rows. Understanding the dynamic interactions between turbines, wind farms, and the ABL can therefore be beneficial in improving the efficiency of wind farm control approaches. Anticipated increases in wind farm size to meet renewable energy targets will increase the importance of exploiting this understanding to advance wind farm control capabilities. This review discusses approaches for modeling and estimation of the wind farm flow field that have exploited such knowledge to varying degrees in closed-loop control. We focus on power tracking as an example application that will be of critical importance as wind farms transition into their anticipated role as major suppliers of electricity. The discussion highlights the benefits of including the dynamics of the flow field in control and points to critical shortcomings of the current approaches.

Contents

1. INTRODUCTION

The United States (1) and European Union (2) have set the ambitious target of net-zero emissions by 2050. In the United States, one part of achieving this emissions reduction objective is attaining a carbon-free electricity system by 2035 (1). These goals will require the dramatic expansion of electricity transmission, energy storage, and renewable resources such as wind energy. As renewable generation displaces traditional power plants, renewable energy providers, such as wind farms, must become more responsive to power system reliability and stability needs (3, 4). Wind farms of the future will therefore require advanced controls that increase power production, reduce mechanical loads, and improve integration within the electric grid. An important part of this integration is the ability to track a power signal trajectory in order to maintain the supply-demand balance dictated by the laws of physics that govern the electric power grid.

Meeting these needs will also require larger wind farms spanning long distances due to the low surface area to power density ratio of wind energy. The large size of modern turbines and the spatial extent of modern wind farms lead to coupling between the performance of the wind farm and the turbulent atmospheric boundary layer (ABL), whose flow produces the kinetic energy driving power production. Turbulence in this lowest level of the atmosphere can be thought of as a random process that has a particular spatial and temporal structure. The characteristics of turbulent air flow through wind farms, sketched in Figure 1, have been well reviewed (5, 6). Turbulent fluctuations in wind speed induce significant variability in wind turbine loading and power generation. The drag force of the ground on the ABL produces an average wind speed that increases with vertical height z. This wind shear produces a variation in the loading on the rotating blades and generates turbulent structures, known as eddies, of various sizes and strength. These eddies are transported downwind at the speed of the wind itself through advection. The largest of these structures are streaks of low and high-speed winds, which are aligned with the streamwise (flow) direction x and meander in the spanwise direction y near the surface of the ground.

The characteristics of the turbulent ABL lead to strong spatio-temporal correlations in power output between turbines (7, 8), which pose a continuing challenge for wind farm control. Streamwise aligned turbines have significant correlations in power output that are largest at the inter-turbine travel time. For staggered wind farms, an additional anti-correlation occurs between staggered rows. The power spectrum of ABL turbulence and the spatio-temporal correlations in wind farms generates a wind farm power spectrum with large fluctuations at low frequencies (8). These fluctuations are significant even for wind farms with hundreds of turbines spread over large areas spanning many kilometers (9, 10).

Wind turbines' energy extraction generates regions of reduced wind speeds downwind, known as wakes. Wakes reduce the power output of downwind turbines, and generate additional turbulence that increases both loading on downwind turbines and the wind travel time between turbines. Wakes nonlinearly interact with each other and the surrounding flow. Turbulence mixes the wakes with the surrounding air as they move downwind, reducing their magnitude and increasing their size, see Figure 1. This weakening of the wakes leads to kinetic energy regeneration for downstream turbines. Wind farms also interact with ABL turbulence and this aerodynamic coupling between wakes, and the turbulent ABL adds another layer of complexity (5, 6), which impacts power output throughout the farm. Advances in wind farm controls, particularly for large farms, is therefore interrelated with advances in understanding the dynamic interactions between turbines, wind farms, and the ABL (11, 12).

An increasing focus on large winds farms, where aerodynamic coupling between turbines is substantial, has prompted additional effort on increasing wind farm power production by modifying wind turbine operating setpoints and layouts (13, 14). In this realm, physical insights into the interaction of wind turbines with the turbulent ABL has played an important role (5). However, the nonlinear interactions between wind turbines and the ABL continues to pose challenges for control algorithms (15), particularly those that require power output regulation (trajectory tracking) at similar time scales to the time it takes a particle of fluid to travel through the entire wind farm (this time is referred to as a wind farm flow through time) (16). While the coupling poses many challenges, it can also provide opportunities for flow control approaches that exploit the flow physics to increase total power output or improve power tracking performance, see e.g. (17, 18, 19, 16, 20, 21).

The primary applications of closed loop control in wind farms are power maximization and power output regulation (tracking) control. Many of these build on well established

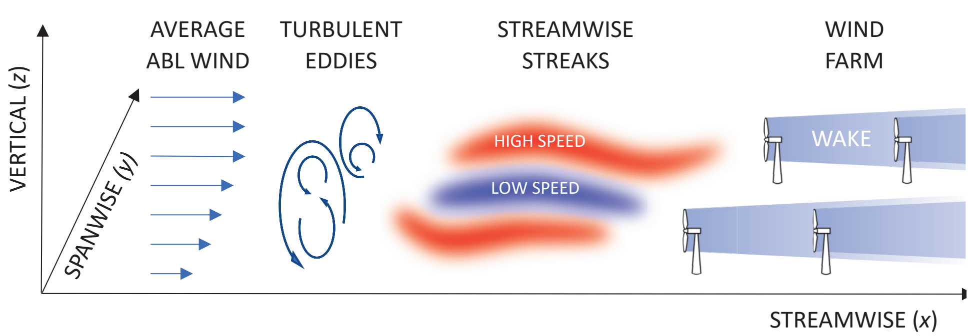

Figure 1

Interactions between the turbulent ABL and wind farms. The turbulent ABL is characterized by a vertically varying average wind speed (wind shear), turbulent eddies, and meandering streamwise streaks of high and low speed winds. Wind farms are affected by the spatio-temporal characteristics of the ABL and modify the flow by generating regions of reduced wind speeds, wakes, that meander and interact with the ABL and each other.

research in controls for individual turbines, see e.g. the reviews in (22, 23, 24), but farm level control requires approaches that consider aerodynamic interactions. These interactions can either reduce or increase power output potential, see e.g. (13, 16, 17). Early wind farm control designs focused on power output maximization. Continuing work in this area employs approaches ranging from simple look up tables (25, 13) to closed loop extrema seeking and proportional integral (PI) control designs, see e.g. (26, 27, 28, 29, 30). Yaw control to maximize power output is another growing area of research (31, 32, 13, 25).

However, new control problems arise as turbines grow rapidly larger and contribute a greater percentage of the electricity supply. For example, the growing size of the turbines is driving greater interest in load reduction through aerodynamic control actuation. Here the current approaches range from lookup table designs (33) to more advanced methods. Wake meandering has been observed as a major source of mechanical loading, and efforts are underway to damp wake meandering for load reduction (34, 35, 36, 37). Mechanical loading throughout wind farms is also highly variable because upstream turbines experience stronger winds and downstream turbines experience larger turbulent fluctuations. Addressing this variability through aerodynamic actuation to equalize loading across wind turbines without affecting power output is a topic of emerging research (33, 38, 39).

In order to meet the grid integration challenges associated with supplying a larger proportion of the energy powering the electric grid, wind farms will need to provide controllable power that ensures stable operations of the power grid. Controllers that reduce the turbulence-induced fluctuations in the power output of a wind farm (40) have been developed in an effort to meet this need. Another area that has received attention in the last few years is the participation of wind farms in ancillary services. Although wind farms have not traditionally participated in these services, their growing percentage of the electricity supply has motivated the development of this new class of controllers to enhance wind farm integration into the power system (41, 42, 43). These control designs aim to reduce the need for the integration of storage and other resources to accommodate renewable energy. Tracking a power reference signal sent by the transmission system operator (TSO) is a particularly important generator capability that regulates the grid's operating frequency by matching power generation and electrical load. The complex interactions between wind farms and the turbulent ABL pose challenges for this type of power tracking control, because the time scales of these reference signals are comparable to the time scales of the wind farm dynamics (turbulence and wake dynamics) and wind farm flow through times.

This review paper outlines some of the modeling and estimation techniques that are enabling closed loop control of wind farms, with a focus on those directed toward power tracking control for grid services. Section 2 discusses the types of existing turbine level control that can be viewed as leveraging the actuation authority in wind farms to control power output through manipulation of the velocity field within the wind farm. This introduction is followed by a discussion of high-fidelity based simulation studies that point to the large potential of this type of flow control in achieving farm level performance goals. Section 3 reviews control oriented models and estimation techniques that have been proposed for real-time control approaches that strive toward achieving the demonstrated potential of control with full information described in Section 2.2. Section 3.3 discusses closed loop control approaches for a power tracking application, and highlights an example approach that combines the flow modeling and estimation techniques to improve the overall efficiency of the control. The paper concludes with a discussion of future research needs.

2. THE PROMISE OF WIND FARM CONTROL

The nonlinear interactions between wind farms and the turbulent ABL pose significant challenges for controlling the power output of wind farms to meet the needs of a changing power system. The dynamic actuation of wind turbines to modify the characteristics of the ABL also presents significant opportunities. In this section we discuss studies that have demonstrated the promise of wind farm control through approaches ranging from static gain scheduling to maximize power output to dynamic optimization based approaches for power tracking.

2.1. A flow control perspective

Wind turbines can be viewed as flow actuators that adjust the strength and direction of their wakes to achieve desired flow conditions (e.g. velocity) for downstream turbines. There are a number of different ways in which a turbine can be controlled. Three common approaches are shown in Figure 2. Induction control (illustrated in the left panel) modulates the trust coefficient C_T, which controls how much kinetic energy is extracted from incoming wind. This type of control is employed to change the strength of the wake and can be accomplished through changes to the pitch angle β of the blades and the torque applied by the generator T_g (23). The center panel shows rotation of the rotor around the tower, known as yawing, which deflects the wake horizontally and curls the wake downstream (44, 45, 13, 46, 47, 25, 48, 49, 14). The right panel illustrates vertical rotation, known as tilting, which curls and deflects the wake vertically. These approaches can be used individually or in combination. The actions of yawing and tilting can also be emulated through pitch control of individual blades, where the pitch angle for each blade is adjusted based on its azimuthal position (13).

All of the actuation techniques discussed above and many new ones proposed in the literature aim to alter the wake strength or deflect the wake as it evolves downstream. We now present a simple model describing an undeflected wake evolution to provide an illustration of how these different types of actuation can affect the power available to downstream turbines. The Jensen model (or Park model) (50) describes the evolution of the velocity

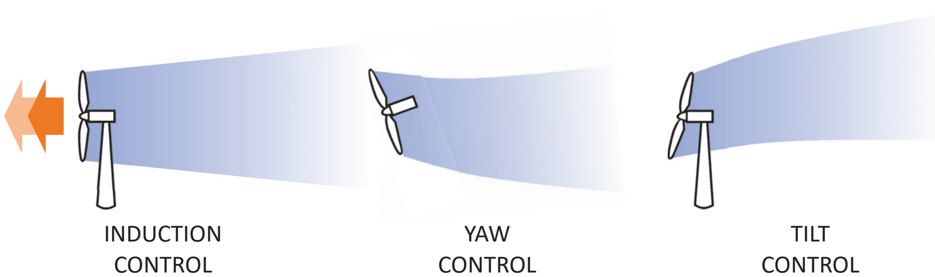

Figure 2

Wake actuation methods for wind farm control include (a) induction control, which changes the strength of the wake, (b) top view of a yawed turbine which leads to spanwise wake deflection (c) a tilted turbine which results in vertical wake deflection. Individual pitch control can also be used to simulate yaw and tilt control without rotating the turbine about the hub.

downstream of a turbine as

$$u(x,r) = U_\infty - \delta u(x) H(x)\, H\left(D_w(x)/2 - r\right) \quad \text{where } \delta u(x) = \frac{2U_\infty a}{D_w^2(x)}, \qquad 1.$$

U_∞ is average upstream wind speed, $\delta u(x)$ is the velocity deficit, $D_w(x) = 1 + 2kx/D$ is the normalized diameter for the wake that expands at a rate k, $H(x)$ is the Heaviside function, and r is the radial distance from the centerline of the wake. The variable a is the induction factor that depends on the thrust coefficient, which can be described by $C_T = 4a(1-a)$ for an ideal un-yawed turbine. Eq. 1. thus describes how the thrust coefficient C_T directly affects the strength of the wake downstream.

The rotor dynamics also affect the turbine power output. The simplest model of a wind turbine is a first order system $J\dot{\omega} = T_a - T_g$, where J is the rotational inertia of the rotor and T_a is the aerodynamic torque (23). The aerodynamic torque $T_a = P_a/\omega$ is set by the aerodynamic power $P_a = \frac{1}{2}\rho\pi R^2 C_P U_\infty^3$, where ω is the rotational speed of the rotor, U_∞ is the average upstream wind speed, ρ is the density of air, and C_P is the aerodynamic power coefficient. For ideal turbines the power coefficient is related to the induction factor, specifically $C_P = 4a(1-a)^2$. However, aerodynamic losses reduce the power coefficient from this optimal value in real turbines. Both the thrust and power coefficients in real turbines therefore depend on the pitch angle β and tip speed ratio $\lambda = \omega R/U_\infty$, where $R = D/2$ is the radius of the swept area of the rotor. However, these relationships differ in that the power coefficient has a single maximum and the thrust coefficient generally increases with increasing pitch angle and tip speed ratio.

The wind turbine's generator provides an opportunity to store or discharge energy stored in the rotational kinetic energy of the rotor (41, 51, 40); however, rotational kinetic energy storage and discharge affects the power and thrust through the tip speed ratio. This type of control provides additional actuation authority in wind farm applications, but the effect of wind turbine control actions on the strength of its wake has additional implications for wind farm control designs. In particular, developing controllers that select the correct generator torque and pitch angle for induction control requires consideration of the tradeoffs in power generation and energy storage in the kinetic energy of the rotor (52, 53, 54, 55).

In the case of yawed or tilted wind turbines, the power and thrust coefficients are further modified by the yaw or tilt angle γ. The effect of this modification is still of considerable debate (56) with power and thrust coefficients differing from the unyawed or untilted coefficient by a factor $\cos^p \gamma$, where the measured value of p depends on the study. Tremendous advances in understanding the aerodynamics of yawed and tilted wind turbines (57, 58, 59, 60), including the deflection and deformation of the wake, has significantly increased the prospect of control. For example, a recent lifting line model demonstrated that the initial deflection speed of the wake $v = \frac{1}{4} C_T U_\infty \cos^2\gamma \sin\gamma$ depends on the thrust coefficient and yaw or tilt angle (57). A model of the shed vorticity from this lifting line can also be used to model the deformation of the wake (60, 58).

2.2. Quantifying the Potential of Wind Farm Control

The aerodynamics of induction pitch control are well established and our understanding of the effects of yaw and tilt actions continues to advance. However, our ability to quantify the overall potential of these actuation techniques for increasing or controlling wind farm power remains a pressing challenge. Validation of wind farm control approaches requires a wind farm testbed (plant model) that captures the full physical mechanisms that govern the

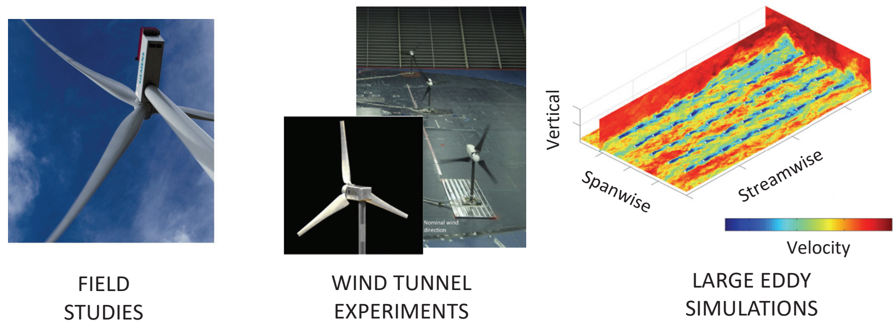

Figure 3

High-quality wind farm plant models (testbeds) include field studies, wind tunnel experiments, and large eddy simulations. Figures adapted from (66, 67, 68, 69); (CC-BY-4.0).

aerodynamics and turbulence in wind farms (61). Field studies, wind tunnel experiments, and high-fidelity simulations, which are each depicted in Figure 3, all provide such a platform but each has its relative benefits and limitations. Evaluations in full-scale wind farms can be deployed effectively (46, 25, 62), but such tests are limited by their expense and complicated by varying operating conditions. Wind tunnel experiments, where the wind turbine is scaled down to fit into a controlled testing environment, have also been used to evaluate the potential of wind farm control (14, 44, 63, 21). However, these experiments are often expensive and complete dynamic scaling is difficult (64, 14, 65).

High-fidelity simulations of wind farms (5) provide a tool that is accurate and that allows for well controlled conditions. The most appropriate numerical models are large eddy simulations (LES), which directly simulate the Navier-Stokes equations for the eddy sizes relevant to wind farm power production and loads. A range of wind turbine representations in LES environments that vary in model fidelity (70) are available. The actuator disk model (ADM) treats the wind turbine as a drag disk that exerts a uniform thrust force across the swept area of the rotor. The actuator disk model with rotation (ADM-R) includes the effects of the rotating rotor on the flow. The actuator line model (ALM) further includes the effect of force variations along each blade of the turbine. The choice of wind turbine model must balance the need for accurate wind turbine dynamics against computational cost.

LES and field studies provide a basis for quantifying the potential of static set-point control of wind farms to maximize power output and reduce wake effects. In field studies, yaw control was found to increase power output by 7-47%, depending on the wind speed (25). Similar power increases have also been found in wind tunnel experiments (44). Numerical simulations found power increases of 4-7% for yaw and tilt-based control (71). The accuracy of high-fidelity simulations avoids erroneous conclusions that can be drawn from low-fidelity models. For example, a number of studies based on engineering models like the Jensen model found that wind farms could increase power production by reducing the induction factor at upstream turbines. However, validation in high-fidelity simulations provided little evidence of this improved power production (72, 65, 14, 73, 74, 75, 76).

High-fidelity numerical simulations also provide a means of exploring the maximum potential of wind farm control because perfect information about the wind flow and

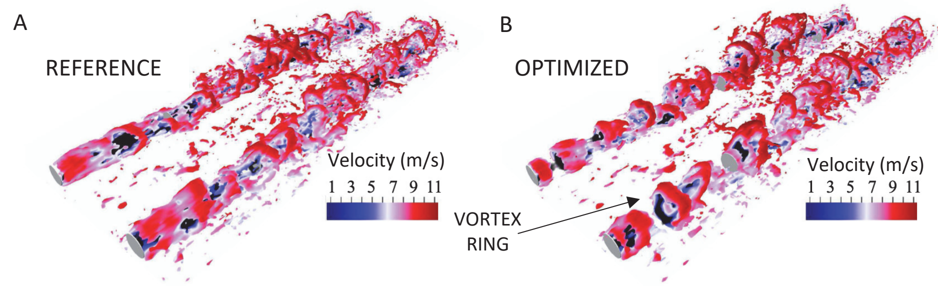

Figure 4

Wind farm velocity field for (A) reference and (B) optimized control. Vortex rings generated in optimized control increase overall wind farm power output by increasing wake mixing. Figure adapted from (79); (CC-BY-4.0).

wind turbine control states are readily available. The work of Goit, Munters, and Meyers (77, 69, 78, 79, 17) exploits this setting to provide fundamental insights into the dynamic potential of wind farm control. In these studies, model predictive control (MPC) with perfect information from LES is used to maximize the power of the wind farm. MPC employs a model to predict and optimize the operation of the wind farm (e.g. maximize power output) over a finite time horizon T. These scheduled, optimized control inputs are used for a finite period $\tau < T$ while a new control signal is computed based on updated measurements. In the nonlinear wind farm control context, the MPC control problem is typically formulated as a constrained optimization problem that is solved using some kind of gradient descent method. As a result, the MPC implementation requires the calculation of analytic gradients of the MPC control model using adjoint equations or automatic differentiation.

In the work of Goit, Munters, and Meyers (77, 69, 78, 79, 17), MPC is implemented using analytically derived adjoint equations for LES and tested using induction and yaw control. These studies found that power can be increased by 6-21% with induction control (77, 69, 78), 21% with yaw control (17), and 25-34% with combined induction and yaw control (17). In power tracking applications, De Rijcke et al. (40) showed a wind turbine's rotational dynamics can reduce turbulence-induced fluctuations in the wind farm power output of their LES. Since these MPC simulations assume perfect knowledge of the wind states and plant dynamics, these results represent potential upper bounds on the realizable power generation increases from this type of approach.

MPC approaches obtained using the LES as the controller model provide additional insight into potential control techniques for increasing power generation. Most notably, (79) noted that the induction control MPC increases power by periodically modulating the thrust coefficient of each turbine. The result of this actuation is to generate vortex rings that increase wake mixing with the surrounding air, as shown in Figure 4, thus reducing the detrimental effects of wakes on downstream turbine power generation.

The perfect information studies described above demonstrate the potential of wind farm control to increase or regulate power production. In the following section we explore emerging modeling, estimation, and control techniques for realizing the potential demonstrated by field, wind tunnel, and LES studies.

3. TOWARD REAL-TIME WIND FARM CONTROL

The results of the last section demonstrate the type of wind farm control that is possible with a high-fidelity wind farm model like LES. However, the computational time of traditional LES prohibits its use as a model for real-time applications. Furthermore, these approaches assume perfect knowledge of the wind states, which is impossible in practice. Recent work in low-order models, sensing and measurements, and state and parameter estimation are enabling real-time control that has the potential to realize a degree of the promise discussed above. A wide range of reduced-complexity models have been developed. They are typically combined within a feedback loop equipped with estimation methods that augment the information available and reduce modeling errors. In this section, we first review some of the prominent modeling approaches. We then briefly discuss some prominent sensing, estimation, and error correction techniques that are combined with these models to improve their fidelity. Finally, we examine application of these techniques to the problem of wind farm power output tracking and highlight the benefits of incorporating aspects of the flow dynamics in this setting.

3.1. Dynamic and control oriented wind farm models

There have been a number of approaches to developing low-order models for both wind farm design and control applications. The closest in resolution to the high-fidelity methods discussed in Section 2.2 are LES run at very coarse grid resolutions, approaching the size of the wind turbine. The coarse grid reduces the computation times by three orders of magnitude over traditional LES (80). Moreover new computational methods are enabling close to real-time simulation (80, 81), which may enable their use in future control applications. These methods have the benefit of capturing the nonlinear response of the wind farm to control actions, see a sample flow field in Figure 5(a), but there is a potential for large errors due to the under-resolution of the flow physics.

Reynolds-Averaged Navier Stokes (RANS) based models aim to reduce complexity over traditional LES by calculating an ensemble-averaged velocity field (82, 83, 84). These models account for the effect of dynamic wind turbine operations and turbulence on the expectation of the velocity field, but do not capture realization specific fluctuations from turbulence. As such, they produce a less detailed flow field, as illustrated in Figure 5(b). RANS based models see computational performance gains similar to the computationally efficient coarse grid LES discussed above (82).

Order-reduction of the LES equations has also been proposed through data-driven system identification techniques such as proper orthogonal decomposition (POD) and dynamic mode decomposition (DMD) (86, 85, 87, 88, 89, 90, 32). POD represents the velocity field $\boldsymbol{u}(\boldsymbol{x}, t)$ through basis functions $\boldsymbol{\psi}(\boldsymbol{x})$ that are ordered by their energy. The number of basis functions is then truncated to achieve a reduced-order model. A DMD model is a data-driven approximation of a Koopman decomposition (91) that instead decomposes the flow into basis functions (modes) associated with distinct harmonics, each associated with a frequency (92, 93). A DMD model then provides a linear map describing the evolution the observed variable (typically the flow field). Both methods reduce the order of the flow field, see e.g., the sample response in Figure 5(c) for comparison to course LES and RANS based approaches. Furthermore, data-driven approaches like DMD and POD are appealing because they do not require detailed knowledge of the complex flow physics. The order reduction enabled through these approaches also provides the potential for real-time computation for control designs, but both approaches have shortcomings in terms of their applicability to control problems. POD models require an extension to a time-dependent setting, see e.g. (94, 95, 86, 89). DMD based models naturally capture the time evolution, but efforts that employ these modes to capture the evolution of the flow field under actuation have been limited (85). Moreover, capturing the nonlinear interactions between the turbulent ABL and a wind farm (whose local behavior is rapidly changing through control actions) tends to require a large number of basis functions, thus increasing the model order. In addition, both POD and DMD based methods tend to require a large amount of data for model identification (96). This data requirement increases in control applications where recalculation is needed due to changes in parameters at each linearization point (97) corresponding to changes in the operating point (flow field) due to control actions.

Linear constant parameter and linear parameter varying models obtained through linearization around operational points have also been proposed as control oriented models (98, 99, 100, 37). These approaches have shown promise in closed loop control applications when combined with sensing and estimation techniques (101). These approaches also benefit from well-developed methods in linear systems and control theory. However, to-date there has been less testing of these approaches within wind farm testbeds that include the dynamics of the turbulent ABL (97). The scalability of these approaches as the number of operating points increases through control actions is also an open question.

Another class of low-complexity models that has shown some potential for real-time control design are dynamic adaptations of steady-state engineering wind farm design models like the Jensen model, described in Eq. 1. The simplest take the form of tracer models that are used to impose turbulence-induced dynamics, as illustrated as Figure 5(a). The most

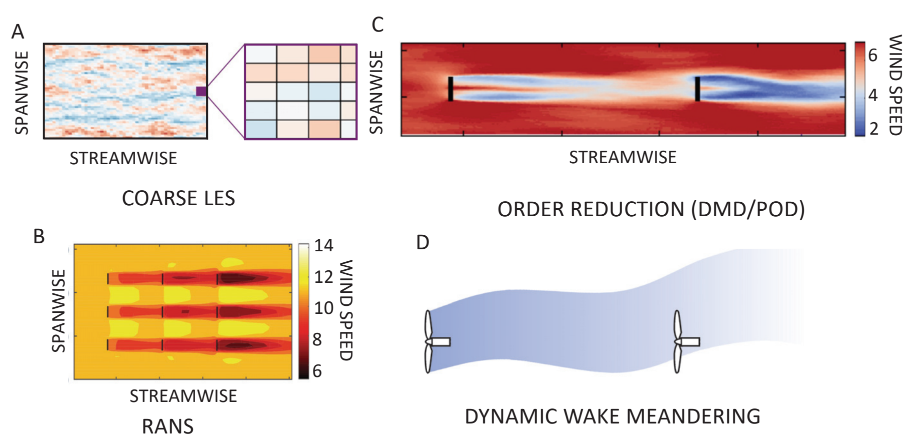

Figure 5

The range of control-oriented models appropriate for wind farm control designs. (A) Coarse LES, where large scales of turbulence are captured and the simulation grid is small enough to simulate in real time. Figure adapted with permission from (80, Figure 1). (B) RANS models, where dynamic effects from wind farm operations and the influence of turbulence are captured in the ensemble-averaged velocity field. Figure adapted from (83) (CC-BY-4.0). (C) Order reduction of LES using DMD, POD, or other methods. Figure adapted with permission from (85, Figure 6 top panel) (©2016 IEEE). (D) Dynamic models, including adaptations of steady-state models, PDE models, or the dynamic wake meandering model.

common of these is the dynamic wake meandering model (102). Time delay adaptations, which assume the wake travels at the upstream velocity U_∞, are also often used (103). Extensions of the Jensen model can also take the form of a partial differential equation model for the reduced wind speed $\delta u(x,t)$ in the wake (18)

$$\frac{\partial \delta u}{\partial t} + U_\infty \frac{\partial \delta u}{\partial x} = -w(x)\delta u(x,t) + f(x,t), \tag{2.}$$

where $w(x)$ is a function that describes the expansion of the wake through turbulent mixing and $f(x,t)$ is a function that represents the wind turbine thrust forcing.

An alternative approach instead views the farm as a graph whose interconnection structure is defined through the wake interactions. In this formulation, the turbines are represented as nodes of the graph and the individual wake interactions between turbines define the edges. Two examples of such graph representations for a five turbine wind farm arranged in a staggered configuration are shown in Figure 6, where panel (a) shows an undirected graph and panel (b) illustrates a directed graph. The undirected representation has proven useful in algorithms to determine the freestream wind direction from noisy turbine measurements (104), while directed graphs are typically employed in models where the wind inlet direction is specified. The directed graph structure then depends on the incoming wind direction and the atmospheric conditions, which enter into the wake expansion rate (as illustrated through the wakes with a linear expansion rate used to determine the connection structure in Figure 6(b)). The farm can then be partitioned into a series of directed subgraphs with the freestream turbine acting as a leader (parent node) and all of the child nodes determined through the wake interactions as the flow travels through the farm. The graph connections are usually determined a priori using farm geometry and wake expansion behavior based on the wind conditions, but recent work that identifies the structure from measured power correlations suggests the promise of this approach in real-time control applications (27).

The graph model also provides a simplified setting for modeling changes in power output due to changes in inlet wind direction, which can be difficult to account for in wake models that typically assume a fixed domain with a known flow direction. Recent work developed such a model employing edge weights defined in terms of inter-turbine wake interaction intensity and time delays to capture the propagation of wind direction changes through the farm (105). A delay dependent adjacency matrix was then used to combine the effect of deficits across a given graph through the linear relation

$$\boldsymbol{\delta u} = U_\infty \mathbf{A}\boldsymbol{\phi}, \tag{3.}$$

where $\mathbf{A}$ is the adjacency matrix defined by the turbine interconnections (graph edges), and $\boldsymbol{\phi}$ captures the deficit relationships between each pair of connected turbines. The graph model implementation described here represents a preliminary attempt at a trade-off between the complexity of the nonlinear approaches discussed above and a linear modeling framework, albeit with the added complexity of the discontinuities in the graph description. In particular, the graph can exhibit edge switching because the turbines in the farm are either connected or not and this connectivity can change with wind farm conditions (e.g., inlet velocity, turbulence intensity or wind direction). Edge switching is particularly challenging to incorporate in optimization problems (106) and related control approaches. However a major benefit of the representation of the farm as a graph that can be partitioned into subgraphs is that it naturally lends itself to distributed computations, which can ameliorate some of the computational challenges associated with real-time control applications.

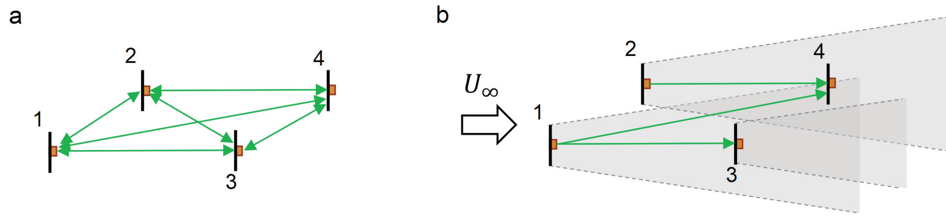

Figure 6

Examples of graph structures for (a) an undirected graph for sensor consensus and (b) a directed graph based on the turbine wakes and current wind direction U_∞, indicated with an arrow.

The graph view can provide a complement to the wake modeling approaches discussed above, particularly in regards to defining the turbines whose wakes interact. A graph-based approach may have advantages in a distributed control setting as only the relationships between turbines are modeled rather than the whole velocity field, which can lead to efficiency improvements, see e.g. (107, 108, 101). This paradigm can be integrated with a dynamic model that can, for example, account for changes to wind inlet direction through a time-dependent change in the graph structure, which overcomes the difficulty and computational expense of implementing a dynamic wind change in models that have a fixed domain such as LES, RANS, or data-driven models trained for a single inlet condition. The effect of dynamically changing wind direction also poses difficultly in a one-dimensional models such as Eq. 2., which inherently assumes a single flow direction. An important direction for future work is the combination of these approaches wherein, e.g., this type of one-dimensional model governs the dynamics along a given edge.

In the next section we describe how estimation techniques can be used to improve the fidelity of all of these models within a control setting.

3.2. Wind farm state and parameter estimation methods

The control-oriented models described in the previous section span a wide range of complexity levels. The type of model best suited will depend on the application, but all of these models make simplifying assumptions about the full flow field that the wind farm is operating within or neglect the uncertainty present in real world conditions. A number of state and parameter estimation approaches have proven effective in at least partially accounting for this uncertainty by combining sensor data with models ranging in fidelity from LES to engineering models, see e.g. (81, 109, 110, 111).

Wind turbines and farms are equipped with a range of sensing capabilities that offer varying levels of accuracy (23). Turbine rotational speed and power output measurements are readily available and typically quite accurate. Anemometers provide wind speed measurements at the rotor, but the outputs are often noisy and can be distorted by aerodynamic interactions with the turbine blades, nacelle, and tower. Strain gauges, torque transducers, and position encoders provide additional information about wind turbine operating conditions (23). Met towers, when installed at hub height, can also provide wind speed and direction data (23).

Lidars provide a more comprehensive measurement of the flow field. Scanning lidar scan

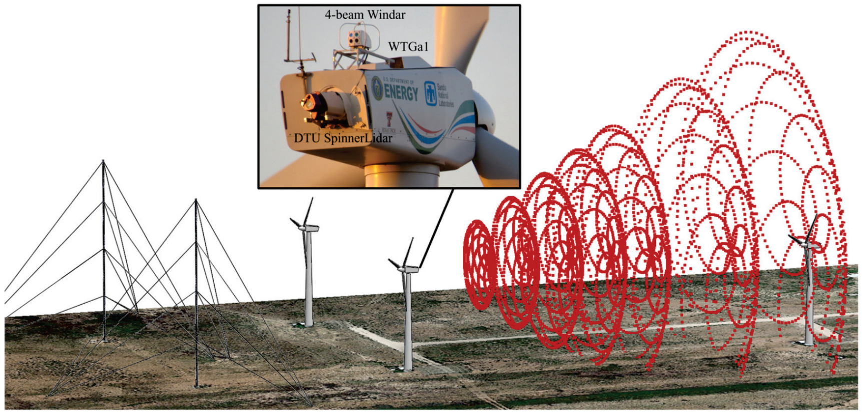

Figure 7

Scanning lidar pattern path of lidar observer attached to a modern wind turbine. Red dots show discrete sampling locations of the lidar with an expanded rosette pattern used to efficiently sample the wake behind the turbine. Figure adapted from (112); (CC-BY-3.0).

a fixed periodic path up or downstream of the wind turbine (112), as shown in Figure 7. The resulting measurement outputs are a weighted velocity along the line of sight of the radar at time-varying locations. Since the scanning frequency of lidars is typically much faster than the dynamics of the turbulent wind flow, lidar is well suited for upstream wind speed measurements for use in feedforward controllers (113, 114) as well as measurements of wake location (115) for use in wake deflection control (116).

A number of state and parameter estimation methods have been employed to incorporate these sensing approaches into low-complexity models. Variations of the Kalman filter are perhaps the most popular. Traditional Kalman filters can be easily applied to linear low-order models (88, 87, 117) and these approaches have been enhanced through Baysian gain tuning algorithms (118). A wide range of Kalman filters, such as extended, approximate, and unscented filters, have been applied to medium fidelity nonlinear RANS models to predict the entire flow field and parameters such as the inflow wind speed and turbulence from SCADA data and lidar (119, 120). Models with a larger state-space are instead often combined with an Ensemble Kalman filter (EnKF), which approximates the error covariance matrix with an ensemble of models thereby reducing the computational burden of computing the Kalman gain matrix (121, 120, 111, 42). Both Extended and EnKF augmented with the dynamics of engineering models have been shown to effectively reduce modeling error between wind farm power predictions and measurements in high-fidelity simulations (122, 123, 109, 42).

Variational state and parameter estimation methods commonly used in atmospheric modeling (124), e.g., 4D-Var, have also shown promise in wind farm applications (125, 110, 81, 126). In these methods a cost functional is minimized while constrained by continuous

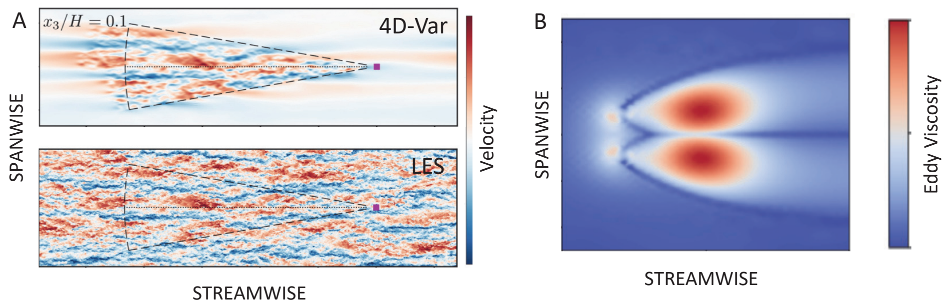

Figure 8

(A) Velocity field reconstruction upstream of turbine using 4D-Var and lidar in LES. Figure adapted with permission from (81, Figure 6(e)(f)). (B) RANS model parameter, eddy viscosity, estimation using 3D-Var. Figure adapted with permission from (110, Figure 2, middle right panel); (©2018 IEEE)

time and/or state space models leading to an optimization problem of the form

$$\min \quad \|\mathbf{y} - \hat{\mathbf{y}}\| + \mathcal{R} \qquad 4.$$

$$\text{subject to} \quad \mathcal{B}(\mathbf{x}) = \mathbf{0} \qquad 5.$$

$$\mathbf{y} = f(\mathbf{x}), \qquad 6.$$

where $\mathbf{x}$ are the states, $\mathbf{y}$ are the outputs, $\hat{\mathbf{y}}$ are the output measurements, $\mathcal{B}(\mathbf{x}) = \mathbf{0}$ are the continuous state space models, $\mathcal{R}$ are regularizations, and $\|\cdot\|$ is a suitable norm. These problems can be solved efficiently using various methods including adjoint equations (110, 81) or through distributed optimization approaches such as alternating direction method of multipliers (ADMM) (126).

Coupling 4D-Var with LES for the state variable equations captures three-dimensional and temporal effects in the estimation. When applied to lidar data, this approach allows for efficient reconstruction of an upstream turbulent velocity field that satisfies the Navier Stokes equations, an example field is shown in Figure 8. The same approach can be applied using RANS models (110) to produce an averaged flow field, as shown in Figure 8. Other state and parameter estimation approaches similarly make use of physical knowledge of the spatio-temporal structure of turbulent velocity variations (115, 113, 114).

3.3. Closed loop control: An example application

We now demonstrate the application of the modeling and estimation techniques discussed in the previous two sections, to a power tracking problem. In particular, we consider the problem of tracking a regulation reference signal

$$P_{\mathrm{ref}}(t) = P_0 + \Delta P r(t) \qquad 7.$$

composed of a baseline power P_0 and a fluctuating power signal whose magnitude is ΔP and trajectory $r(t) \in [-1, 1]$. A baseline strategy in which each turbine maximizes its own power output is often referred to as "greedy control" and leads to a total farm power output $P_{\mathrm{greedy}}(t)$. In order to provide power tracking, the wind farm must reduce the baseline power generation to less than the average of the greedy power output, also known as derating. As a result, the typical choice is to set $P_0 + \Delta P \leq \bar{P}_{\text{greedy}}$, where $\bar{P}_{\text{greedy}}$ is a time average of the greedy power output. Turbulent fluctuations have a strong influence on the derate that is required since the available power to the wind farm will fluctuate around $\bar{P}_{\text{greedy}}$.

The use of derating has significant economic implications because wind farms are compensated by the TSO for both the amount of energy provided to the power grid through the bulk power market, i.e. $\int P_{\text{ref}}(t)\,dt$, and the amount of regulation power provided to the power grid, i.e. ΔP. As a result, wind farms that derate their baseline power generation sacrifice revenue from bulk power production that may not be recovered through ancillary service payments (127). The development of wind farm controllers that can reduce derates or otherwise maximize revenue is a growing area of concern as wind farms increase their role on the power grid.

Individual wind turbine controllers can derate their baseline power generation by reducing the power coefficient through pitch or generator torque actuation (41). Since a number of solutions exist for a given derated power coefficient, the controller can be tuned to store kinetic energy in the rotating rotor (41). In the case of wind farms, standard wind turbine control strategies are not directly applicable in power tracking applications because power coefficient derating modifies the strength and characteristics of wakes, and alters downstream power output potential. For example, (16) and (128) showed in LES that when wind turbine level control approaches are applied to each wind turbine in a farm, the wind farm is unable to track a power reference signal. As a result, new control designs must be developed that account for wake interactions.

A simple and effective approach was developed by (43) that uses a proportional-integral (PI) controller to distribute the reference signal to each wind turbine in the farm. This model-free approach allows turbines operating below the maximum power point to increase production to compensate for turbines that cannot increase their power output. The control is implemented using induction control, where the thrust coefficient actuation is used as a proxy for blade pitch angle and generator torque actuation, and validated in LES. Vali et al. (129, 128) noted that since a number of solutions to the power tracking problem exist, the PI controller can be turned to select setpoints that also reduce the dynamic loading on the turbines. Although the PI control approach is elegant in its simplicity and absence of a controller model, these controllers are designed to operate within the range of reference signals where $P_0 + \Delta P \leq \bar{P}_{\text{greedy}}$, i.e. the derate is greater than equal to the power reference signal magnitude and less overall wind power is produced.

Boersma et al. (130, 131) proposes a power tracking design comprising two control loops. The inner loop tracks the power reference signal and minimizes loads through induction control using MPC built around a static wake model. The outer loop adjusts the yaw setting to allow the wind farm to track up-regulation signals that could not be tracking using induction control alone. By yawing the upstream turbines, the controller reduces wake effects and increases the available power. Perfect knowledge is assumed for the observer, and the design is tested in LES. This approach has negative economic implications similar to the controller by (43) where wind farms sacrifice considerable energy payments in order to provide regulation. As wind farm operators begin to implement yaw controllers to increase power production the increased power generation of yaw-optimized wind farms will become the standard. However, this control approach will prevent wind farm operators from realizing the power production gains of yaw control to increase the farm's baseline power production as the yaw actions are instead directed toward providing regulation through

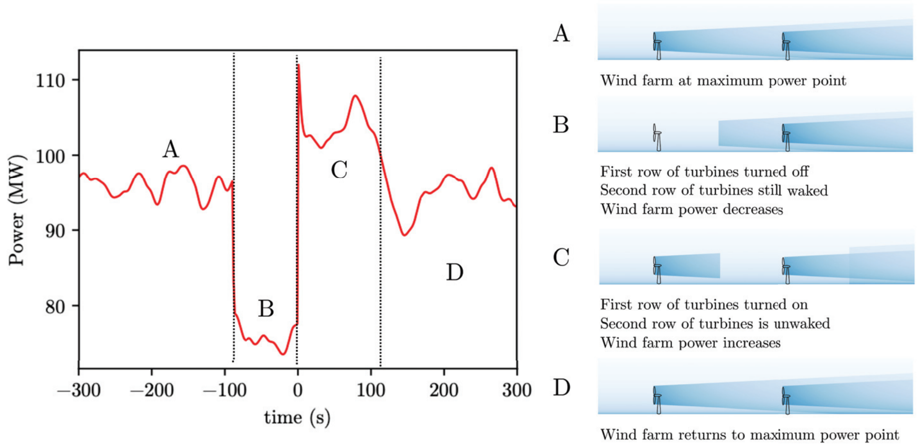

Figure 9

Example of wind farm power modulation (left) via aerodynamic storage and extraction of wind kinetic energy with the wake strength (right) shown in blue during four time periods. The wind farm (A) begins at the steady-state maximum power point with power fluctuations caused by atmospheric turbulence. At $t = -90$ s (B) the first row of turbines is turned off, moving kinetic energy extraction at the first row to (C) the second row where power production surges. Wind farm power output returns (D) to the steady-state maximum. Left panel adapted with permission from (132, Figure 1); (©2020 IEEE).

power tracking.

Dynamic model-based control designs that directly take into account the aerodynamics within the farm interactions have shown the potential of taking advantage of the flow physics to reduce the required derate (42). In particular, models that account for wake advection (inter-turbine travel time for a particular parcel of fluid) can take advantage of aerodynamic energy storage within large wind farms. This form of storage is generated by reducing power extraction at upstream turbines resulting in lesser wakes and an associated velocity field with higher energy extraction potential that can be extracted at a later time when that fluid arrives at given downstream location.

To more clearly demonstrate this aerodynamic storage mechanism, consider the simple on-off control shown in Figure 9 (132). In this simple case, the wind farm begins at the steady-state maximum power point with power fluctuations caused by atmospheric turbulence. At $t = -90$s, the the first row of turbines is turned off, reducing the power output of the farm considerably. After the wind travels through the wind farm, kinetic energy extraction that had been occurring at the first row takes place at the second row at $t = 0$s. If the wind turbines at the first row are turned on at the same time, the power production of the entire farm surges. Eventually, the wake of the first row returns and the power production of the farm returns to the steady-state maximum power point. This case demonstrates that energy can be stored in the flow field of the wind farm. The efficiency of the storage is 40–80%, depending on the spacing of the turbines, and the time scale of the storage is simply the farm length divided by the wind speed, and as such can be significant for large wind farms.

A low-complexity model combined with a range of state and parameter estimation

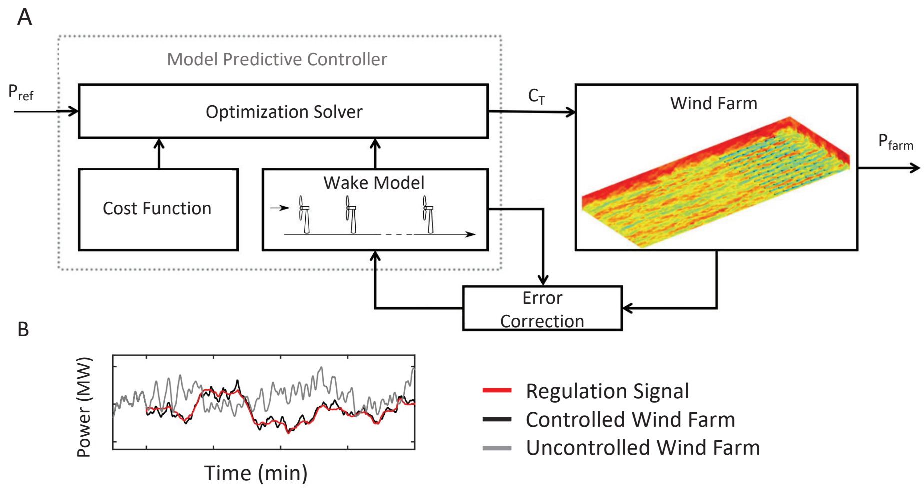

Figure 10

(A) Block diagram of wind farm controller designed to track a power reference signal for power tracking. Top panel adapted with permission from (42, Figure 1); (©2017 John Wiley and Sons).. (B) Power output of controlled wind farm when tested with TSO reference signal. Bottom panel adapted with permission from (18, Figure 8 bottom left panel); (©2017 IEEE)

methods formed the basis for a closed-loop model predictive controller that took advantage of this type of storage to achieve power tracking (18, 19, 42). That work focused on frequency regulation control, which is a grid support service wherein a generator (in this case the wind farm) is controlled to track a power reference signal sent by the TSO, P_{ref}. The controller is built around the dynamic PDE engineering wake model in Eq. 2.. The velocities and wake expansion rates in the model are corrected using power generation measurements that were incorporated into an EnKF. Thrust coefficient actuation is used as a proxy for blade pitch angle and generator torque actuation. A block diagram of the closed loop control is shown in Figure 10. When tested in an LES model, the wind farm was able to track realistic reference signals in many cases with lower derates than traditional approaches with controller computations performed in real-time. Power tracking results are also shown in Figure 10b. These results demonstrate that the controlled wind farm is able to track the reference signal, even in cases where the signal exceeds the power output of the uncontrolled wind farm by taking advantage of the aerodynamic storage capabilities within the wind farm flow field. In this case, the controller selects reduced thrust coefficients at upstream wind turbines in advance of increased power demand to store kinetic energy in the wind farm flow field (55).

This section provides an example control problem using a particular model, but similar MPC approaches relying on a low or medium-fidelity control model have also been developed in recent years. Vali et al. (133) used a RANS model, which can be coupled with an EnKF observer (119) with induction and yaw control. Farm level power tracking by directly controlling generator torque and pitch angle have also been explored (55); however, including the rotor dynamics in the control algorithm greatly increases the complexity of the control problem. While these approaches are promising, testing with high-fidelity plant models is a necessary first step in moving them into practice.

The model-based MPC approaches discussed above provide an important proof of concept in terms of using low-order models for closed loop control of wind farms for this power tracking application. However many of the studies above either assume simple wind farm layouts or small wind farms simple wind farm layouts. As the size of wind farms increase or additional degrees of freedom are added to account for more complex geometry or control approaches, the computational costs associated with MPC based approaches may pose limitations to real-time implementation.

Distributed computation and control approaches attempt to address this issue (107, 108, 101, 134, 135, 136). For example, MPC designs that take advantage of the network structure to compute local control actions within subgraphs associated with the graph modeling paradigm discussed in Section 3.1 can reduce the computational burden by distributing the control computations to each subgraph. This type of distributed model-based MPC framework (101) has shown promise within FLOw Redirection and Induction in Steady State (FLORIS) model, which provides a highly tuned reduced order wind farm simulation platform (137). A consensus algorithm evaluated over a graph structure has also enabled substantial computational reduction in the prediction of wind direction from noisy sensor measurements (104) and short-term power output from SCADA data (126). Continued research in this direction is needed to understand the full potential and possible limitations of these approaches.

4. OUTLOOK

The continuing rapid expansion of wind energy is driving advances in modeling, estimation, and control approaches for wind farms. High-fidelity simulation approaches have illustrated the promise of a wide range of new control modalities that can not only facilitate better integration with the electric power system but also enable wind farms to provide grid services. However, there are wide gaps between these proof of concept simulations and robust implementations in the field. In fact, most of the control approaches proposed have yet to be validated in a high-fidelity plant models with estimation techniques based on available sensor data.

Integration of many proposed control approaches within existing wind turbine control loops also presents a number of challenges. First, many control designs and simulation based studies use variables such as thrust coefficient as a proxy for blade pitch angle and generator torque actuation. The associated mapping from these variables to turbine control loops can be difficult to implement within realistic wind farm testbeds such as LES. Many control objectives can be achieved through multiple actuation strategies, and there have been few studies that combine approaches such as pitch and yaw control, either with one another, or with storage of kinetic energy in the rotors. This integration is complicated by the multiple timescales over which these actions affect the flow field both locally and far downstream. To-date no models fully describe dynamic interactions for a single turbine, let alone within a farm where this greatly complicates wake interactions.

Perhaps the most pressing challenge is limitations in our current understanding of the kinetic energy potential of an incoming flow field. While there is work to estimate the power potential within a given farm for power maximization (138, 139), the problem becomes more difficult in power tracking applications. Characterizing this potential is further complicated by variations in wind direction that occur over the same timescales as wind farm flow through times. The behavior of wind farms under dynamic wind speed and direction changes and representations of this behavior are also under studied.

Finally, observers play a key role in closed-loop wind farm control, but the potential of these observers is not well understood. There is a gap between empirical results suggesting that an output observer can reconstruct important flow data and rigorous characterization of the observability of the flow field, although these studies are starting to be performed (140). Rigorous observability margins would allow control designs to better incorporate sensing and measurements into feedback control and to evaluate the limitations of a given approach.

The challenges listed above underscore the close connection between understanding the dynamics of the turbulent ABL and achieving the full potential of wind farm control. While the challenges are manifold, the societal benefits associated with addressing then underscores the importance of advancing our knowledge to meet them. Advances to bring these emerging applications to fruition will help realize global goals to decarbonize the electric power sector.

SUMMARY POINTS

1. Wind farms and the turbulent atmospheric boundary layer in which they operate are inextricably linked; explicitly accounting for these interactions within control approaches becomes increasingly important as the size of wind farms increases.
2. Control approaches that include flow physics show promising benefits in applications such as power tracking, which motivates continued development of these methods.
3. There has been great progress in a wide range of approaches that combine low-order models and estimation techniques to enable closed-loop wind farm control but challenges remain in moving from proof of concept simulations to real-world implementation.
4. Combining different modeling paradigms, sensing and computational approaches will play a critical role in bridging the gap between research and practice.

FUTURE ISSUES

1. There is a need to bridge the gap between proof of concept control approaches and real-world implementation.
2. Computational approaches that enable higher-fidelity representations under the rapidly changing behavior of a controlled wind farm remain an ongoing challenge.
3. Understanding the kinetic energy potential of the farm is critical to achieving the full potential of wind farm control and enabling wind farms to better support the grid.
4. Understanding the extent to which the available and proposed sensor measurements can enable the required level of observability for real-time control is an ongoing challenge.

DISCLOSURE STATEMENT

The authors are not aware of any affiliations, memberships, funding, or financial holdings that might be perceived as affecting the objectivity of this review.

ACKNOWLEDGMENTS

The authors thank their colleagues and collaborators, P. Bauweraerts, J. Bossuyt, J. Bretheim, R. B. Cal, B. F. Hobbs, M. Howland, L. A. Martinez-Tossas, W. Munters, R. J. A. M. Stevens, V. Thomas, and C. VerHulst, who have contributed to many of the approaches and ideas reviewed here through insightful conversations and joint projects. We are particularly grateful to Charles Meneveau and Johan Meyers who helped initiate our research in this area and Jennifer King whose ongoing collaboration has advanced our understanding. The authors would also like to thank the National Science Foundation who have provided ongoing support (most recently through grant numbers CMMI 1635430, 2034111, CBET 1949778 and DGE-1746891)

LITERATURE CITED

1. The White House. 2021. President Biden takes executive actions to tackle the climate crisis at home and abroad, create jobs, and restore scientific integrity across federal government
2. European Commission. 2020. 2030 Climate target plan
3. Ahlstrom M, Ela E, Riesz J, O'Sullivan J, Hobbs BF, et al. 2015. The evolution of the market: Designing a market for high levels of variable generation. *IEEE Power and Energy Magazine* 13:60–66
4. Kroposki B, Johnson B, Zhang Y, Gevorgian V, Denholm P, et al. 2017. Achieving a 100% renewable grid: Operating electric power systems with extremely high levels of variable renewable energy. *IEEE Power and Energy Magazine* 15:61–73
5. Stevens RJ, Meneveau C. 2017. Flow structure and turbulence in wind farms. *Annual Review of Fluid Mech.* 49:311–339
6. Porté-Agel F, Bastankhah M, Shamsoddin S. 2019. Wind-turbine and wind-farm flows: A review. *Boundary-Layer Meteorology* 174:1–59
7. Bossuyt J, Howland MF, Meneveau C, Meyers J. 2016. Measurement of unsteady loading and power output variability in a micro wind farm model in a wind tunnel. *Experiments in Fluids* 58
8. Stevens RJAM, Meneveau C. 2014. Temporal structure of aggregate power fluctuations in large-eddy simulations of extended wind-farms. *J. Renewable and Sustainable Energy* 6:043102
9. Apt J. 2007. The spectrum of power from wind turbines. *J. Power Sources* 169:369–374
10. Bandi MM. 2017. Spectrum of wind power fluctuations. *Physical Review Letters* 118
11. Veers P, Dykes K, Lantz E, Barth S, Bottasso CL, et al. 2019. Grand challenges in the science of wind energy. *Science* 366:eaau2027
12. Meneveau C. 2019. Big wind power: Seven questions for turbulence research. *J. Turbulence* 20:2–20
13. Fleming P, Gebraad PM, Lee S, van Wingerden JW, Johnson K, et al. 2014. Simulation comparison of wake mitigation control strategies for a two-turbine case. *Wind Energy* 18:2135–2143
14. Campagnolo F, Petrovic V, Bottasso CL, Croce A. 2016. *Wind tunnel testing of wake control strategies*. In *2016 American Control Conference (ACC)*, pp. 513–518. Piscataway, NJ: IEEE
15. Boersma S, Doekemeijer B, Gebraad P, Fleming P, Annoni J, et al. 2017. *A tutorial on control-*

oriented modeling and control of wind farms. In *2017 American Control Conference (ACC)*, pp. 1–18. Piscataway, NJ: IEEE
16. Fleming P, Aho J, Gebraad P, Pao L, Zhang Y. 2016. *Computational fluid dynamics simulation study of active power control in wind plants*. In *2016 American Control Conference (ACC)*, pp. 1413–1420. Piscataway, NJ: IEEE
17. Munters W, Meyers J. 2018. Towards practical dynamic induction control of wind farms: Analysis of optimally controlled wind-farm boundary layers and sinusoidal induction control of first-row turbines. *Wind Energy Science* 3:409–425
18. Shapiro CR, Bauweraerts P, Meyers J, Meneveau C, Gayme DF. 2017. Model-based receding horizon control of wind farms for secondary frequency regulation. *Wind Energy* 20:1261–1275
19. Shapiro CR, Meyers J, Meneveau C, Gayme DF. 2018. Wind farms providing secondary frequency regulation: Evaluating the performance of model-based receding horizon control. *Wind Energy Science* 3:11–24
20. Frederik JA, Doekemeijer BM, Mulders SP, Wingerden JW. 2020. The helix approach: Using dynamic individual pitch control to enhance wake mixing in wind farms. *Wind Energy* 23:1739–1751
21. Frederik JA, Weber R, Cacciola S, Campagnolo F, Croce A, et al. 2020. Periodic dynamic induction control of wind farms: proving the potential in simulations and wind tunnel experiments. *Wind Energy Science* 5:245–257
22. Barlas T, van Kuik G. 2010. Review of state of the art in smart rotor control research for wind turbines. *Progress in Aerospace Sciences* 46:1–27
23. Pao LY, Johnson KE. 2011. Control of wind turbines. *IEEE Control Systems* 31:44–62
24. Njiri JG, Söffker D. 2016. State-of-the-art in wind turbine control: Trends and challenges. *Renewable and Sustainable Energy Reviews* 60:377–393
25. Howland MF, Lele SK, Dabiri JO. 2019. Wind farm power optimization through wake steering. *Proceedings of the National Academy of Sciences* 116:14495–14500
26. Simley E, Fleming P, King J. 2020. Design and analysis of a wake steering controller with wind direction variability. *Wind Energy Science* 5:451–468
27. Bernardoni F, Ciri U, Rotea M, Leonardi S. 2020. Real-time identification of clusters of turbines. *J. Phys.: Conf. Series* 1618:022032
28. Ciri U, Rotea M, Santoni C, Leonardi S. 2017. Large-eddy simulations with extremum-seeking control for individual wind turbine power optimization. *Wind Energy* 20:1617–1634
29. Johnson KE, Fritsch G. 2012. Assessment of extremum seeking control for wind farm energy production. *Wind Engineering* 36:701–715
30. Bin Salamah Y, Ozguner U. 2021. Distributed extremum-seeking for wind farm power maximization using sliding mode control. *Energies* 14:828
31. Raach S, van Wingerden JW, Boersma S, Schlipf D, Cheng PW. 2017. *H_∞ controller design for closed-loop wake redirection*. In *2017 American Control Conference (ACC)*, pp. 703–708
32. Raach S, Schlipf D, Cheng PW. 2017. Lidar-based wake tracking for closed-loop wind farm control. *Wind Energy Science* 2:257–267
33. Reyes HM, Kanev S, Doekemeijer B, van Wingerden JW. 2019. Validation of a lookup-table approach to modeling turbine fatigue loads in wind farms under active wake control. *Wind Energy Science* 4:549–561
34. Yang Z, Li Y, Seem JE. 2015. Multi-model predictive control for wind turbine operation under meandering wake of upstream turbines. *Control Engineering Practice* 45:37–45
35. Riverso S, Mancini S, Sarzo F, Ferrari-Trecate G. 2017. Model predictive controllers for reduction of mechanical fatigue in wind farms. *IEEE Trans. Control Systems Technology* 25:535–549
36. Singh P, Seiler P. 2017. *Controlling a meandering wake: Insights from full-information control*. In *2017 American Control Conference (ACC)*, pp. 697–702. Piscataway, NJ: IEEE
37. Singh P, Seiler P. 2019. *Controlling the Meandering Wake Using Measurement Feedback*. In *2019 American Control Conference (ACC)*, pp. 4144–4150. Piscataway, NJ: IEEE

38. Zhao R, Shen W, Knudsen T, Bak T. 2012. Fatigue distribution optimization for offshore wind farms using intelligent agent control. *Wind Energy* 15:927–944
39. Bartl J, Ostovan Y, Uzol O, Sætran L. 2017. Experimental study on power curtailment of three in-line turbines. *Energy Procedia* 137:307–314
40. Rijcke SD, Driesen J, Meyers J. 2014. Power smoothing in large wind farms using optimal control of rotating kinetic energy reserves. *Wind Energy* 18:1777–1791
41. Aho J, Buckspan A, Laks J, Fleming P, Jeong Y, et al. 2012. *A tutorial of wind turbine control for supporting grid frequency through active power control*. In *2012 American Control Conference (ACC)*, pp. 3120–3131. Piscataway, NJ: IEEE
42. Shapiro CR, Meyers J, Meneveau C, Gayme DF. 2017. *Dynamic wake modeling and state estimation for improved model-based receding horizon control of wind farms*. In *2017 American Control Conference (ACC)*, pp. 709–716. Piscataway, NJ: IEEE
43. van Wingerden JW, Pao L, Aho J, Fleming P. 2017. Active power control of waked wind farms. *IFAC-PapersOnLine* 50:4484–4491
44. Bastankhah M, Porté-Agel F. 2019. Wind farm power optimization via yaw angle control: A wind tunnel study. *J. Renewable and Sustainable Energy* 11:023301
45. Annoni J, Fleming P, Scholbrock A, Roadman J, Dana S, et al. 2018. Analysis of control-oriented wake modeling tools using lidar field results. *Wind Energy Science* 3:819–831
46. Fleming P, Annoni J, Shah JJ, Wang L, Ananthan S, et al. 2017. Field test of wake steering at an offshore wind farm. *Wind Energy Science* 2:229–239
47. Fleming P, King J, Dykes K, Simley E, Roadman J, et al. 2019. Initial results from a field campaign of wake steering applied at a commercial wind farm – part 1. *Wind Energy Science* 4:273–285
48. Ahmad T, Basit A, Ahsan M, Coupiac O, Girard N, et al. 2019. Implementation and analyses of yaw based coordinated control of wind farms. *Energies* 12:1266
49. Bromm M, Rott A, Beck H, Vollmer L, Steinfeld G, Kühn M. 2018. Field investigation on the influence of yaw misalignment on the propagation of wind turbine wakes. *Wind Energy* 21:1011–1028
50. Jensen NO. 1983. A note on wind generator interaction. Tech. Rep. Risø-M-2411, Risø National Laboratory
51. Ahmadyar AS, Verbic G. 2017. Coordinated operation strategy of wind farms for frequency control by exploring wake interaction. *IEEE Trans. Sustainable Energy* 8:230–238
52. Stotsky A, Egardt B, Carlson O. 2013. *Control of wind turbines: A tutorial on proactive perspectives*. In *2013 American Control Conference (ACC)*. Piscataway, NJ: IEEE
53. Kazda J, Mirzaei M, Cutululis NA. 2018. *On the Architecture of Wind Turbine Control Required for Induction-based Optimal Wind Farm Control*. In *2018 American Control Conference (ACC)*, pp. 3074–3079. Piscataway, NJ: IEEE
54. van der Hoek D, Kanev S, Engels W. 2018. *Comparison of Down-Regulation Strategies for Wind Farm Control and their Effects on Fatigue Loads*. In *2018 American Control Conference (ACC)*, pp. 3116–3121. Piscataway, NJ: IEEE
55. Shapiro CR, Meyers J, Meneveau C, Gayme DF. 2018. *Coordinated pitch and torque control of wind farms for power tracking*. In *2018 American Control Conference (ACC)*, pp. 688–694. Piscataway, NJ: IEEE
56. Howland MF, González CM, Martínez JJP, Quesada JB, Larrañaga FP, et al. 2020. Influence of atmospheric conditions on the power production of utility-scale wind turbines in yaw misalignment. *J. Renewable and Sustainable Energy* 12:063307
57. Shapiro CR, Gayme DF, Meneveau C. 2018. Modelling yawed wind turbine wakes: A lifting line approach. *J. Fluid Mech.* 841:R1
58. Zong H, Porté-Agel F. 2021. Experimental investigation and analytical modelling of active yaw control for wind farm power optimization. *Renewable Energy* 170:1228–1244
59. Bossuyt J, Scott R, Ali N, Cal RB. 2021. Quantification of wake shape modulation and de-

flection for tilt and yaw misaligned wind turbines. *J. Fluid Mech.* 917:A3
60. Martínez-Tossas LA, Annoni J, Fleming PA, Churchfield MJ. 2019. The aerodynamics of the curled wake: A simplified model in view of flow control. *Wind Energy Science* 4:127–138
61. Annoni J, Seiler P, Johnson K, Fleming P, Gebraad P. 2014. *Evaluating wake models for wind farm control*. In *2014 American Control Conference (ACC)*, pp. 2517–2523. Piscataway, NJ: IEEE
62. Bossanyi E, Ruisi R. 2021. Axial induction controller field test at Sedini wind farm. *Wind Energy Science* 6:389–408
63. Petrović V, Schottler J, Neunaber I, Hölling M, Kühn M. 2018. Wind tunnel validation of a closed loop active power control for wind farms. *J. Phys.: Conference Series* 1037:032020
64. Miller MA, Kiefer J, Westergaard C, Hansen MOL, Hultmark M. 2019. Horizontal axis wind turbine testing at high Reynolds numbers. *Physical Review Fluids* 4
65. Bartl J, Sætran L. 2016. Experimental testing of axial induction based control strategies for wake control and wind farm optimization. *J. Phys.: Conference Series* 753:032035
66. Gonzalez AG, Enevoldsen PB, Barlas A, Madsen HA. 2021. Field test of an active flap system on a full-scale wind turbine. *Wind Energy Science* 6:33–43
67. Bartl J, Mühle F, Schottler J, Sætran L, Peinke J, et al. 2018. Wind tunnel experiments on wind turbine wakes in yaw: Effects of inflow turbulence and shear. *Wind Energy Science* 3:329–343
68. Schreiber J, Bottasso CL, Salbert B, Campagnolo F. 2020. Improving wind farm flow models by learning from operational data. *Wind Energy Science* 5:647–673
69. Goit J, Munters W, Meyers J. 2016. Optimal coordinated control of power extraction in LES of a wind farm with entrance effects. *Energies* 9:29
70. Stevens RJAM, Martínez LA, Meneveau C. 2018. Comparison of wind farm large eddy simulations using actuator disk and actuator line models with wind tunnel experiments. *Renewable Energy* 116:470 – 478
71. Fleming PA, Ning A, Gebraad PMO, Dykes K. 2015. Wind plant system engineering through optimization of layout and yaw control. *Wind Energy* 19:329–344
72. Annoni J, Gebraad PMO, Scholbrock AK, Fleming PA, van Wingerden JW. 2016. Analysis of axial-induction-based wind plant control using an engineering and a high-order wind plant model. *Wind Energy* 19:1135–1150
73. Ciri U, Rotea M, Santoni C, Leonardi S. 2016. *Large Eddy Simulation for an array of turbines with Extremum Seeking Control*. In *2016 American Control Conference (ACC)*, pp. 531–536. Piscataway, NJ: IEEE
74. Gebraad P, Fleming P, van Wingerden J. 2015. *Comparison of actuation methods for wake control in wind plants*. In *2015 American Control Conference (ACC)*, pp. 1695–1701. Piscataway, NJ: IEEE
75. van der Hoek D, Kanev S, Allin J, Bieniek D, Mittelmeier N. 2019. Effects of axial induction control on wind farm energy production - a field test. *Renewable Energy* 140:994–1003
76. Kheirabadi AC, Nagamune R. 2019. A quantitative review of wind farm control with the objective of wind farm power maximization. *J. Wind Engineering and Industrial Aerodynamics* 192:45–73
77. Goit JP, Meyers J. 2015. Optimal control of energy extraction in wind-farm boundary layers. *J. Fluid Mech.* 768:5–50
78. Munters W, Meyers J. 2017. An optimal control framework for dynamic induction control of wind farms and their interaction with the atmospheric boundary layer. *Phil. Trans. the Royal Society A: Mathematical, Physical and Engineering Sciences* 375:20160100
79. Munters W, Meyers J. 2018. Dynamic strategies for yaw and induction control of wind farms based on large-eddy simulation and optimization. *Energies* 11:177
80. Bauweraerts P, Meyers J. 2019. On the feasibility of using large-eddy simulations for real-time turbulent-flow forecasting in the atmospheric boundary layer. *Boundary-Layer Meteorology*

171:213–235
81. Bauweraerts P, Meyers J. 2020. Reconstruction of turbulent flow fields from lidar measurements based on large-eddy simulation. *J. Fluid Mech.* 906
82. Boersma S, Gebraad P, Vali M, Doekemeijer B, van Wingerden J. 2016. A control-oriented dynamic wind farm flow model: "WFSim". *J. Phys.: Conference Series* 753:032005
83. Boersma S, Doekemeijer B, Vali M, Meyers J, van Wingerden JW. 2018. A control-oriented dynamic wind farm model: WFSim. *Wind Energy Science* 3:75–95
84. Iungo GV, Viola F, Ciri U, Rotea MA, Leonardi S. 2015. Data-driven RANS for simulations of large wind farms. *J. Phys.: Conference Series* 625:012025
85. Annoni J, Gebraad P, Seiler P. 2016. *Wind farm flow modeling using an input-output reduced-order model*. In *2016 American Control Conference (ACC)*, pp. 506–512. Piscataway, NJ: IEEE
86. Annoni J, Seiler P. 2015. *A low-order model for wind farm control*. In *2015 American Control Conference (ACC)*, pp. 1721–1727. Piscataway, NJ: IEEE
87. Fortes-Plaza A, Campagnolo F, Wang J, Wang C, Bottasso C. 2018. A POD reduced-order model for wake steering control. *J. Phys.: Conference Series* 1037:032014
88. Iungo GV, Santoni-Ortiz C, Abkar M, Porté-Agel F, Rotea MA, Leonardi S. 2015. Data-driven reduced order model for prediction of wind turbine wakes. *J. Phys.: Conference Series* 625:012009
89. VerHulst C, Meneveau C. 2014. Large eddy simulation study of the kinetic energy entrainment by energetic turbulent flow structures in large wind farms. *Phys. Fluids* 26:025113
90. Hamilton N, Tutkun M, Cal RB. 2016. Low-order representations of the canonical wind turbine array boundary layer via double proper orthogonal decomposition. *Phys. Fluids* 28:025103
91. Mezić I. 2005. Spectral properties of dynamical systems, model reduction and decompositions. *Nonlinear Dynamics* 41:309–325
92. Schmid PJ. 2010. Dynamic mode decomposition of numerical and experimental data. *J. of Fluid Mech.* 656:pp 5–28
93. Rowley CW, Mezić I, Bagheri S, Schlatter P, Henningson DS. 2009. Spectral analysis of nonlinear flows 641:115–127
94. Hamilton N, Viggiano B, Calaf M, Tutkun M, Cal RB. 2018. A generalized framework for reduced-order modeling of a wind turbine wake. *Wind Energy* 21:373–390
95. Debnath M, Santoni C, Leonardi S, Iungo GV. 2017. Towards reduced order modelling for predicting the dynamics of coherent vorticity structures within wind turbine wakes. *Phil. Trans. of the Royal Society of London A: Mathematical, Physical and Eng. Sciences* 375
96. Zhang M, Stevens RJAM. 2020. Characterizing the coherent structures within and above large wind farms. *Boundary-Layer Meteorology* 174:61–80
97. Cassamo N, van Wingerden JW. 2021. *Model Predictive Control for Wake Redirection in Wind Farms: A Koopman Dynamic Mode Decomposition Approach*. In *2021 American Control Conference (ACC)*, pp. 1772–1778. Piscataway, NJ: IEEE
98. Boersma S, Vali M, Kuhn M, van Wingerden JW. 2016. *Quasi Linear Parameter Varying modeling for wind farm control using the 2D Navier-Stokes equations*. In *2016 American Control Conference (ACC)*, pp. 4409–4414. Piscataway, NJ: IEEE
99. Annoni J, Howard K, Seiler P, Guala M. 2015. An experimental investigation on the effect of individual turbine control on wind farm dynamics. *Wind Energy* 19:1453–1467
100. Buccafusca L, Jansch-Porto JP, Dullerud GE, Beck CL. 2019. An application of nested control synthesis for wind farms. *IFAC-PapersOnLine* 52:199–204
101. Bay CJ, Annoni J, Taylor T, Pao L, Johnson K. 2018. *Active Power Control for Wind Farms Using Distributed Model Predictive Control and Nearest Neighbor Communication*. In *2018 American Control Conference (ACC)*, pp. 682–687. Piscataway, NJ: IEEE
102. Larsen GC, Madsen HA, Thomsen K, Larsen TJ. 2008. Wake meandering: A pragmatic approach. *Wind Energy* 11:377–395

103. Gebraad PMO, van Wingerden JW. 2014. A control-oriented dynamic model for wakes in wind plants. *J. Phys.: Conference Series* 524:012186
104. Annoni J, Bay C, Johnson K, Dall'Anese E, Quon E, et al. 2019. Wind direction estimation using scada data with consensus-based optimization. *Wind Energy Science* 4:355–368
105. Starke GM, Stanfel P, Meneveau C, Gayme DF, King J. 2021. *Network based estimation of wind farm power and velocity data under changing wind direction*. In *2021 American Control Conference (ACC)*, pp. 1799–1806. Piscataway, NJ: IEEE
106. Rogozin A, Uribe CA, Gasnikov AV, Malkovsky N, Nedić A. 2020. Optimal distributed convex optimization on slowly time-varying graphs. *IEEE Trans. Control of Network Systems* 7:829–841
107. Annoni J, Bay C, Taylor T, Pao L, Fleming P, Johnson K. 2018. *Efficient Optimization of Large Wind Farms for Real-Time Control*. In *2018 American Control Conference (ACC)*, pp. 6200–6205. Piscataway, NJ: IEEE
108. Annoni J, Dall'Anese E, Hong M, Bay CJ. 2019. *Efficient Distributed Optimization of Wind Farms Using Proximal Primal-Dual Algorithms*. In *2019 American Control Conference (ACC)*, pp. 4173–4178. Piscataway, NJ: IEEE
109. Gebraad P, Fleming P, van Wingerden J. 2015. *Wind turbine wake estimation and control using FLORIDyn, a control-oriented dynamic wind plant model*. In *2015 American Control Conference (ACC)*, pp. 1702–1708. Piscataway, NJ: IEEE
110. Adcock C, King RN. 2018. *Data-Driven Wind Farm Optimization Incorporating Effects of Turbulence Intensity*. In *2018 American Control Conference (ACC)*, pp. 695–700. Piscataway, NJ: IEEE
111. Doekemeijer B, Boersma S, Pao L, van Wingerden J. 2018. Joint state-parameter estimation for a control-oriented LES wind farm model. *J. Phys.: Conference Series* 1037:032013
112. Herges TG, Keyantuo P. 2019. Robust lidar data processing and quality control methods developed for the SWiFT wake steering experiment. *J. Phys.: Conference Series* 1256:012005
113. Laks J, Simley E, Pao L. 2013. *A spectral model for evaluating the effect of wind evolution on wind turbine preview control*. In *2013 American Control Conference (ACC)*, pp. 3673–3679. Piscataway, NJ: IEEE
114. Simley E, Pao L. 2013. *Reducing LIDAR wind speed measurement error with optimal filtering*. In *2013 American Control Conference (ACC)*, pp. 621–627. Piscataway, NJ: IEEE
115. Raach S, Schlipf D, Haizmann F, Cheng PW. 2014. Three dimensional dynamic model based wind field reconstruction from lidar data. *J. Phys.: Conference Series* 524:012005
116. Dhiman H, Deb D, Muresan V, Balas V. 2019. Wake management in wind farms: An adaptive control approach. *Energies* 12:1247
117. Sinner M, Pao LY, King J. 2020. *Estimation of Large-Scale Wind Field Characteristics using Supervisory Control and Data Acquisition Measurements*. In *2020 American Control Conference (ACC)*, pp. 2357–2362
118. Moustakis N, Mulders SP, Kober J, van Wingerden JW. 2019. *A Practical Bayesian Optimization Approach for the Optimal Estimation of the Rotor Effective Wind Speed*. In *2019 American Control Conference (ACC)*, pp. 4179–4185. Piscataway, NJ: IEEE
119. Doekemeijer BM, van Wingerden JW, Boersma S, Pao LY. 2016. Enhanced Kalman filtering for a 2D CFD NS wind farm flow model. *J. Phys.: Conference Series* 753:052015
120. Doekemeijer BM, Boersma S, Pao LY, Knudsen T, van Wingerden JW. 2018. Online model calibration for a simplified LES model in pursuit of real-time closed-loop wind farm control. *Wind Energy Science* 3:749–765
121. Doekemeijer BM, Boersma S, Pao LY, van Wingerden JW. 2017. *Ensemble Kalman filtering for wind field estimation in wind farms*. In *2017 American Control Conference (ACC)*, pp. 19–24. Piscataway, NJ: IEEE
122. Knudsen T, Bak T, Soltani M. 2011. Prediction models for wind speed at turbine locations in a wind farm. *Wind Energy* 14:877–894

123. Knudsen T, Bak T. 2013. *Simple model for describing and estimating wind turbine dynamic inflow*. In *2013 American Control Conference (ACC)*, pp. 640–646. Piscataway, NJ: IEEE
124. Kalnay E. 2003. *Atmospheric modeling, data assimilation, and predictability*. Cambridge New York: Cambridge University Press
125. Cherukuru NW, Calhoun R, Krishnamurthy R, Benny S, Reuder J, Flügge M. 2017. 2D VAR single doppler lidar vector retrieval and its application in offshore wind energy. *Energy Procedia* 137:497–504
126. Annoni J, Bay C, Johnson K, Fleming P. 2019. *Short-Term Forecasting Across a Network for the Autonomous Wind Farm*. In *2019 American Control Conference (ACC)*, pp. 2837–2842. Piscataway, NJ: IEEE
127. Rose S, Apt J. 2013. The cost of curtailing wind turbines for secondary frequency regulation capacity. *Energy Systems* 5:407–422
128. Vali M, Petrović V, Steinfeld G, Pao LY, Kühn M. 2019. An active power control approach for wake-induced load alleviation in a fully developed wind farm boundary layer. *Wind Energy Science* 4:139–161
129. Vali M, Petrović V, Steinfeld G, Pao LY, Kühn M. 2018. Large-eddy simulation study of wind farm active power control with a coordinated load distribution. *J. Phys.: Conference Series* 1037:032018
130. Boersma S, Doekemeijer B, Keviczky T, van Wingerdenl J. 2019. *Stochastic Model Predictive Control: Uncertainty impact on wind farm power tracking*. In *2019 American Control Conference (ACC)*, pp. 4167–4172. Piscataway, NJ: IEEE
131. Boersma S, Doekemeijer B, Siniscalchi-Minna S, van Wingerden J. 2019. A constrained wind farm controller providing secondary frequency regulation: An LES study. *Renewable Energy* 134:639–652
132. Shapiro CR, Ji C, Gayme DF. 2020. *Real-time energy market arbitrage via aerodynamic energy storage in wind farms*. In *2020 American Control Conference (ACC)*, pp. 4830–4835. Piscataway, NJ: IEEE
133. Vali M, Petrović V, Boersma S, van Wingerden JW, Pao LY, Kühn M. 2019. Adjoint-based model predictive control for optimal energy extraction in waked wind farms. *Control Engineering Practice* 84:48–62
134. Gionfra N, Sandou G, Siguerdidjane H, Faille D, Loevenbruck P. 2019. A discrete-time PID-like consensus control: Application to the wind farm distributed control problem. In *Informatics in Control, Automation and Robotics*. Springer International Publishing
135. Ebegbulem J, Guay M. 2017. Distributed extremum seeking control for wind farm power maximization. *IFAC-PapersOnLine* 50:147–152
136. Siniscalchi-Minna S, Bianchi FD, Ocampo-Martinez C, Domínguez-García JL, Schutter BD. 2020. A non-centralized predictive control strategy for wind farm active power control: A wake-based partitioning approach. *Renewable Energy* 150:656–669
137. NREL. 2020. FLORIS. Version 2.2.3. *GitHub repository*
138. Göçmen T, Giebel G, Poulsen NK, Sørensen PE. 2018. Possible power of down-regulated offshore wind power plants: The PossPOW algorithm. *Wind Energy* 22:205–218
139. Siniscalchi-Minna S, Bianchi FD, De-Prada-Gil M, Ocampo-Martinez C. 2019. A wind farm control strategy for power reserve maximization. *Renewable Energy* 131:37–44
140. Doekemeijer B, Wingerden JW. 2020. Observability of the ambient conditions in model-based estimation for wind farm control: A focus on static models. *Wind Energy* 23:1777–1791